Accuracy of GPR based 3D fracture surface geometry interpretation

R. Kiuru[1], P. Kantia[2], L. Uotinen[1] & M. Janiszewski[1]

[1]*Aalto University School of Engineering, Department of Civil Engineering, Espoo, Finland*
[2]*Geofcon (Kantia Oy), Rovaniemi, Finland*

* risto.kiuru@aalto.fi

Introduction

In the past decade, various nuclear waste management organizations have put significant effort into developing methods that can identify and characterize excavation damaged zone (EDZ) around hard rock excavations (Heikkinen et al., 2010). Much of this research has been centered around the use of ground penetrating radar (GPR) to detect fractures parallel to the tunnel profile in the first metres below the excavated surface (Heikkinen & Kantia, 2011; Mattila et al., 2015). Accuracy of the EDZ interpretation is largely affected by the capabilities of GPR to identify said fractures, and to establish their orientation. In order to verify the performance of GPR in this context, a set of tests was carried out on mostly homogeneous Kuru grey granite from Kuru, Tampere, Finland.

GPR survey

Three slabs of 1 x 1 metre in size and with a thickness of approximately 400 mm were sawcut from intact rock blocks of Kuru granite. These slabs were carefully split approximately at the middle while avoiding excessive damage to the sides of the specimens. This resulted in three specimens with an artificially induced fracture surface. The specimens were then measured using a GPR antenna with a central frequency of 1600 MHz. For each specimen, a total of 18 scanlines (9 in the X-direction and 9 in the Y-direction) were measured with a line spacing of 100 mm. Along the scanlines a total of 200 traces/m were recorded with 2048 samples per trace. This data was then processed to create 2D profiles of the fracture surface location in respect to the specimen surface (Fig. 1). When converting from time to distance, an observed median value of 4.8 (Kiuru & Kantia, 2020) was used for the relative dielectric permittivity of Kuru grey granite.

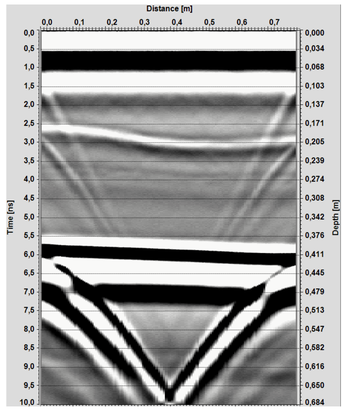

Figure 1. *Example of the obtained GPR data for specimen RAKKA-1. Reflections from the fractures surfaces are clearly seen in the GPR data (A). Thickness of the slab varies slightly, which can be seen in the tilted reflection from the backplate (B). Data is in respect to the top surface.*

Photogrammetry

After the GPR measurements, the top slab was carefully lifted, rotated and placed on a revolving platform for capturing of the true fracture geometry using photogrammetry (Fig. 2). The photographs were taken using Canon 5DS R DSLR camera and Canon 35 mm f/1.4L II USM objective. The camera was held in place using a tripod and the slab was rotated 8.4 degrees between the photographs from dip angles of 30, 45 and 60 degrees resulting in a total of 129 photographs. The photogrammetric modelling and automatic scaling using distance marker were carried out in RealityCapture 1.0.3.9696 software. Further processing and rotation and translation of the point clouds were done using CloudCompare 2.10.1 software. The vertical position of the fracture surface was obtained as two raster X-Y grids with unit dimensions of 1 mm x 1 mm and 0.5 mm x 0.5 mm. Each point in the grid represents the mean height of the points inside the grid square.

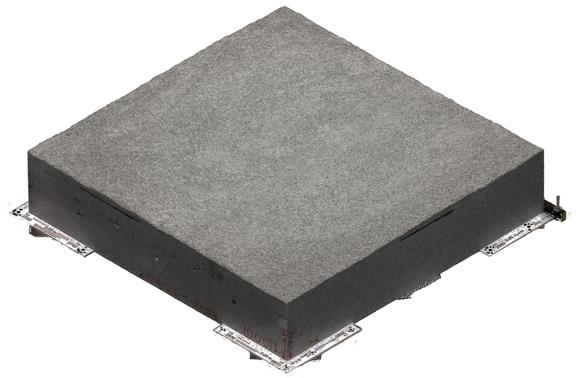

Figure 2. *Example of the obtained photogrammetric model for specimen RAKKA-1. Opened fracture surface facing up, topside facing down. Origin of the coordinate system is at the topside corner at the bottom of the image. Distance markers can be seen in the corners of the slab.*

Comparison and results

Finally, the results from GPR measurements were compared to the photogrammetrically obtained fracture surface geometry to establish the accuracy of the GPR based fracture surface geometry interpretation. This was done by downsampling both datasets to 10 mm in the X and Y directions and comparing the Z values point-by-point. To account for uncertainty in the relative dielectric permittivity values, the GPR measurements were calibrated based on the cumulative distributions of fracture locations. In general, the GPR survey captures the larger scale geometry of the fracture surface to a reasonable degree (Fig. 3). Mean deviations of the GPR interpretations from the photogrammetrically obtained fracture locations were 2.36 mm, 2.33 mm and 2.70 mm with standard deviations of 1.98 mm, 1.70 mm and 2.34 mm for RAKKA-1, RAKKA-2 and RAKKA-3, respectively (Fig. 4). With respect to the mean fracture depths of 191 mm, 205 mm and 187 mm this works out to 1.24 %, 1.14 % and 1.44 % for RAKKA-1, RAKKA-2 and RAKKA-3, respectively.

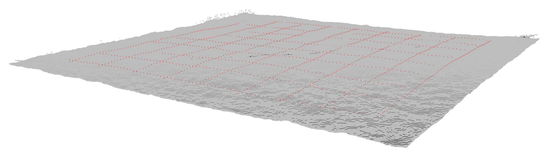

Figure 3. *Photogrammetric model of the fracture surface (grey) of specimen RAKKA-1 and fracture locations as interpreted from the GPR survey, downsampled to 10 mm (red). Visualised with Rhino 6.*

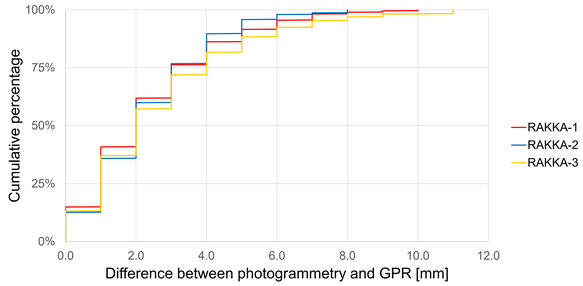

Figure 4. *Absolute values of the deviations of the GPR interpretations from the photogrammetrically obtained fracture surfaces for specimens RAKKA-1, RAKKA-2 and RAKKA-3. Data downsampled to 10 mm. Line spacing of GPR 100 mm. Total number of compared points 1193 (RAKKA-1), 1110 (RAKKA-2) and 1117 (RAKKA-3).*

References:

Kiuru, R. and Kantia, P., 2020. *Attenuation of ground penetrating radar signal in Kuru granite.* Conference proceedings of the ISRM International Symposium EUROCK 2020 – Hard Rock Engineering in Trondheim, Norway 14.-19.6.2020.

Mattila, J. et al., 2015. *Parametrisation of Fractures - Characterisation of Potential Target Structures.* Posiva Oy, Working Report 2015-26.

Heikkinen, E. and Kantia, P., 2011. *Suitability of Ground Penetrating Radar for Locating Large Fractures.* Posiva Oy, Working Report 2011-92.

Heikkinen, E. et al., 2010. *EDZ Assessments in Various Geological Environments Using GPR Method.* Posiva Oy, Working Report 2010-4.

Acknowledgements

We would like to thank Academy of Finland for funding (grants 297770 and 319798).

More information:

eng.aalto.fi/en